

## Ferromagnetic Resonance of Supported Nickel with Adsorbed Hydrogen, Oxygen, and Ethylene

A. A. ANDREEV\* AND P. W. SELWOOD

*From the Department of Chemistry, University of California,  
Santa Barbara, California*

Received May 23, 1967

Ferromagnetic resonance (FMR) spectra have been obtained for silica-supported nickel in several mean particle sizes, and both before and after the chemisorption of hydrogen, oxygen, and ethylene. The results are in general agreement with previously reported studies on these systems by classical methods. The FMR method is more sensitive than the classical by several orders of magnitude. It also gives more information concerning, especially, the magnetocrystalline anisotropy and the surface anisotropy, and the manner in which these are changed by adsorbed molecules.

Classical magnetic methods have contributed to the understanding of chemisorption on nickel (1, 2), but the use of magnetic resonance in this area has thus far been limited (3, 4). Ferromagnetic resonance (FMR) has not only greater sensitivity than the classical constant-field or low-frequency AC permeameter methods, but it affords opportunities for more detailed investigation of electronic interaction between adsorbate and metal surface.

Permeameter studies on nickel (5, 6) have shown the effect of adsorbed oxygen on both the saturation magnetic moment and on the ferromagnetic anisotropy. By applying the techniques of electron spin resonance to this and related systems it is possible to observe changes in the moment, the magnetocrystalline anisotropy, and the surface anisotropy. In this paper FMR measurements are reported for finely divided nickel as adsorbent for hydrogen, oxygen, and ethylene.

### EXPERIMENTAL

The FMR spectra were recorded with a Varian V-4502 X-band EPR spectrometer

\* Present address: Institute of Organic Chemistry, Bulgarian Academy of Science, Sofia, Bulgaria.

with 100-ke/sec field modulation. A variable temperature accessory permitted measurements between  $-150^{\circ}$  and  $300^{\circ}\text{C}$ . A suitable vacuum device and "quick-disconnect coupling" of the wave guide allowed reduction of the samples *in situ*, and measurement of the equilibrium pressure of the gaseous adsorbate. The lowest pressure attainable was about  $1 \times 10^{-6}$  mm Hg. The use of West Glass greaseless high-vacuum stopcocks, and a trap cooled with liquid nitrogen, minimized any influence of mercury and grease vapors. During the experiments on ethylene the trap was cooled to  $-76^{\circ}\text{C}$ . The sample holder was in the form of a slender silica vacuum trap.

Hydrogen was purified by passing it through an Engelhard Deoxo unit and then over silica gel at  $-196^{\circ}\text{C}$ . In some of the experiments hydrogen diffused through palladium-silver was used. Oxygen was obtained by decomposition of previously evacuated potassium permanganate. Phillips research grade ethylene was used.

Two different silica-supported nickel samples were employed. Sample No. 1 was prepared by homogeneous hydrolysis of nickel nitrate solution on Davison silica gel as described by van Eijk van Voorthuijsen and Franzen (7) according to their prepara-

tion No. 8252. This sample contained 14.8% nickel, and the mean diameter of the nickel particles according to X-ray linewidth broadening was 36 Å. This sample was reduced in flowing hydrogen for 20 hr at 400°C, then evacuated for 4 hr at 360°C. Sample No. 2 was prepared by mixing boiling sodium metasilicate and sodium carbonate solution with boiling nickel nitrate solution according to ref. (7), No. 5421. This sample contained 36.2% nickel, and the nickel particles had a mean diameter of 60 Å. The sample was reduced for 20 hr at 390°C and evacuated for 4 hr at 360°C. The usual sample mass was 0.05 g.

### RESULTS AND DISCUSSION

In this section results and comments will be presented *seriatim* on the bare nickel and then for each of the adsorbates. The magnetic resonance absorption of nickel, as a typical ferromagnetic, is very large. The first FMR experiment was performed with nickel metal (8).

**Bare nickel.** Figures 1 and 2 show the magnetization, linewidth, and  $g$  value for Samples 1 and 2, as a function of temperature from 25° to 300°C.

In the case of Sample No. 2, which has the larger mean particle diameter, the magnetization varies more steeply with temperature, in agreement with previously reported results of constant-field measurements (9). This agreement is easy to understand because of the proportionality between FMR line intensity and the saturation magnetization of nickel catalyst (10).

Many determinations have been made of ferromagnetic resonance linewidth in nickel single crystals (11–13). Usually the linewidth is between 500 and 1000 gauss, but in nearly perfect crystals the width is much less (13). In polycrystalline samples the linewidth is greater, and typical nickel catalyst samples show a linewidth of from 470 to 1800 gauss (3, 4, 10, 14, 15). The reason for this, as described by Turov (16), is that because of the various directions (and, generally speaking, magnitudes) of the internal anisotropy fields of crystallites oriented in different directions, the resonance curve is spread out—each producing resonance at its own unique value of the external field. Line-broadening in polycrystalline samples is thus an obvious result of magnetic anisotropy.

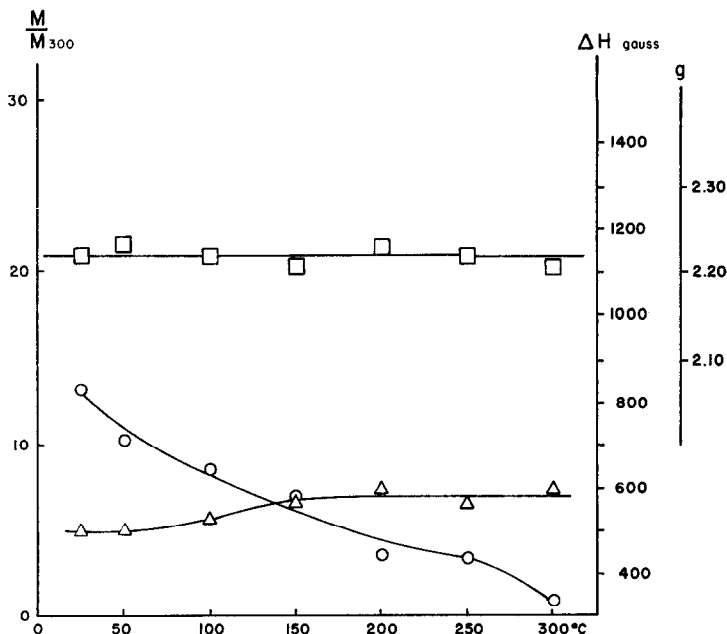


Fig. 1. Temperature dependence of magnetization  $M/M_{300}$ ,  $\circ$ ; linewidth  $\Delta H$ ,  $\triangle$ ; and  $g$  value,  $\square$  for Sample No. 1. Magnetization at 300°C ( $M_{300}$ ) is taken for unit.

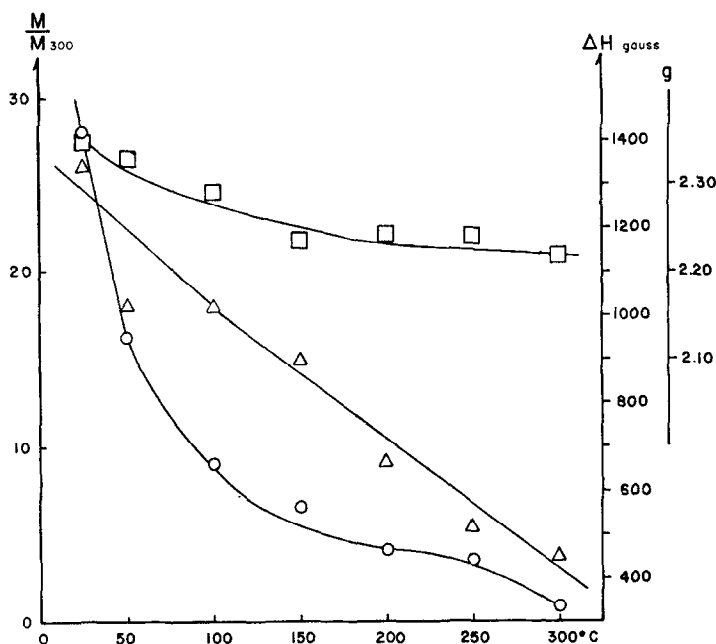


FIG. 2. Temperature dependence of magnetization  $M/M_{300}$ ,  $\circ$ ; linewidth  $\Delta H$ ,  $\triangle$ ; and  $g$  value,  $\square$  for Sample No. 2.

The dependence of linewidth on temperature is different for each sample. Sample No. 2 shows a rapid decrease of linewidth with increasing temperature, while Sample No. 1 shows only a slight increase. In Sample No. 1 there is no evidence for magnetic inhomogeneities—that is to say, no evidence for significant anisotropy—all particles thus behaving as single domains. Resonance then occurs under conditions of uniform magnetization of all metal present. The linewidth observed in such cases can be related mostly to interaction between electrons contributing to ferromagnetism and conduction electrons by a spin-electron relaxation process. But Sample No. 2 in contrast has particles exhibiting nonuniform internal effective magnetic anisotropy, and this is the chief reason for the broader line and the greater temperature dependence of linewidth on temperature. The magnetic anisotropy in particle assemblies of this kind decreases with increasing temperature (16), thus leading to a decreased linewidth. There is no evidence for appreciable dipole-dipole interaction between individual nickel crystallites (17, 18), and the results do not offer any explanation for linewidth and  $g$

values on the basis of a "skin-effect." The particle-size data tend to exclude such a possibility.

Turning now to the  $g$  values, we find many different values from 2.09 to 2.8 in the literature (3, 4, 10, 14, 15). The  $g$  value is very sensitive to particle size, shape, and surface configuration, and is thus sensitive to composition and to manner of preparation and treatment in a typical catalyst preparation.

It is possible to explain the temperature dependence of resonance position in terms of magnetic moment and anisotropy. In a very simple case, for a single crystal with cubic symmetry, when ferromagnetic resonance is observed by applying a magnetic field parallel to the direction of easy magnetization (19), we have  $\omega = \gamma (H + H_A)$ , and  $\Delta H = 2 \alpha (H + H_A)$  where  $\omega$  is the resonance frequency,  $\gamma$  the magnetomechanical ratio,  $H$  the external field in the isotropic case,  $H_A$  the anisotropy field, and  $\alpha$  the Landau-Lifshitz damping parameter. We also have  $H_A = f (K/M_s)$  where  $K$  is the anisotropy constant and  $M_s$  the saturation magnetization.

From Fig. 2 it may be seen that increase

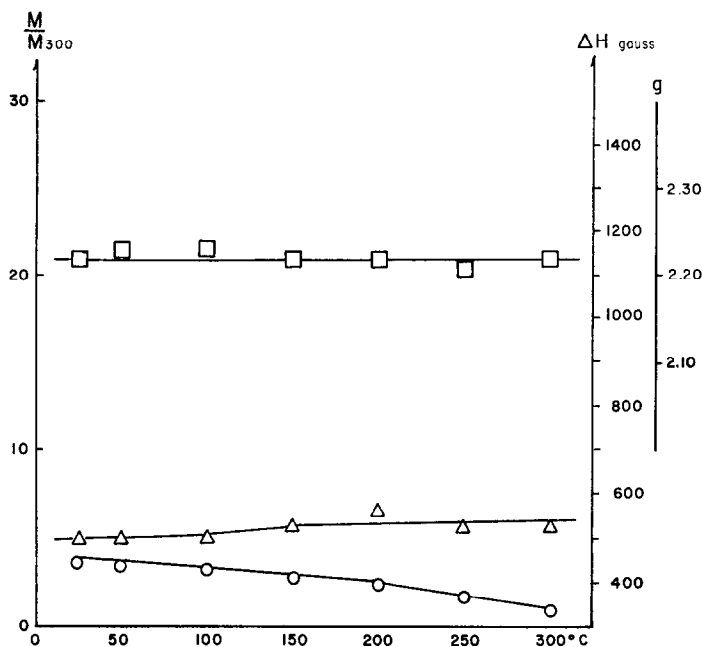


FIG. 3. Temperature dependence of magnetization  $M/M_{300}$ , ○; linewidth  $\Delta H$ , △; and  $g$  value, □ for Sample No. 1 after adsorption of hydrogen at 300°C and  $P(\text{H}_2) = 600$  mm Hg.

of temperature is accompanied by a substantial decrease of  $g$  value, as shown by the increase of external applied field necessary for resonance. (All  $g$  values in this work were calculated from the external applied field for resonance  $H$ , thus  $\omega = \gamma H$ .) The temperature dependence of the external applied field necessary for resonance for Sample No. 2 is in agreement with that reported for nickel whisker and platelet monocrystals with diameters about 800 Å, and thus much larger than the particles in Sample No. 2 (13). But the behavior of Sample No. 1 is quite different and can be explained by the independence of  $K/M_s$  from temperature. This view is supported by the smaller particle size of Sample No. 1 and by its behavior subsequent to the adsorption of gas molecules, as described below.

**Adsorbed hydrogen.** Figures 3 and 4 give the results found after adsorption of hydrogen at 300°C and 600 mm Hg pressure, on Samples Nos. 1 and 2, respectively. The general form of the several curves, as a function of temperature, is in agreement with results obtained from constant-field measurements (9).

For both Samples Nos. 1 and 2 there is a general decrease of linewidth on adsorption of hydrogen. This can be explained by the nickel lattice constant increase after hydrogen adsorption as found by both X-ray (21, 22) and neutron (23) diffraction. An increase of lattice constant must lead to a decrease of dipole-dipole interaction in the crystal and hence a decrease of linewidth. It is noted also that hydrogen adsorption decreases the slopes of the  $\Delta H/T$  and the  $g/T$  plots, as may be seen by comparing Fig. 4 with Fig. 2. This may be explained as due to a decrease of anisotropy in Sample No. 2, after adsorption, as already shown by the earlier permeameter studies (6). For example, in the simplest case  $H_A = 2 K_1/M_s$  and a decrease in  $K_1$  (the first anisotropy constant) will give the effect found. Adsorption has as one of its results a decrease in the number of electron spins participating in resonance, the volume and surface of the remaining ferromagnetic core is diminished, and consequently the anisotropy decreases.

In Figs. 5 and 6 there are shown recorded FMR spectra, for Samples Nos. 1 and 2 respectively, prior to and after the adsorp-

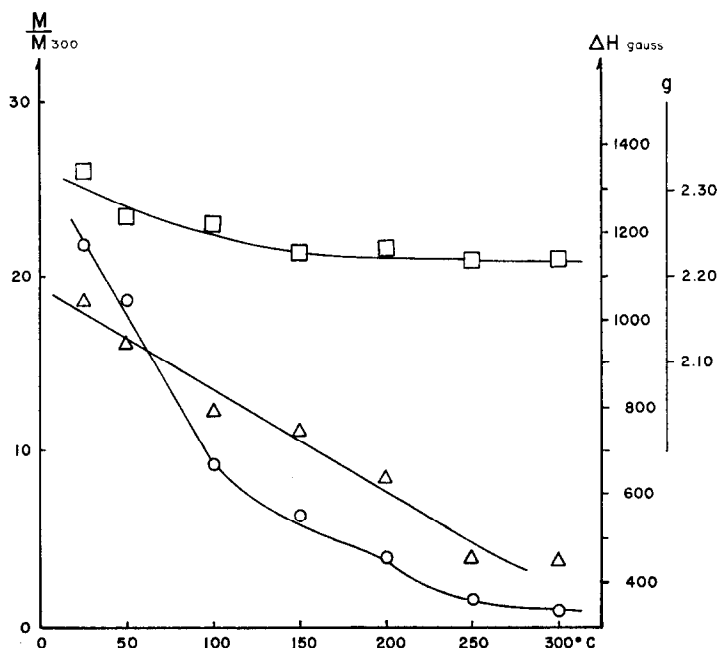


FIG. 4. Temperature dependence of magnetization  $M/M_{300}$ , ○; linewidth  $\Delta H$ , △; and  $g$  value, □ for Sample No. 2 after adsorption of hydrogen at 300°C and  $P(H_2) = 600$  mm Hg.

tion of hydrogen at 25°C and 500 mm Hg. Hydrogen adsorption decreases the magnetization of Sample No. 1, as may be predicted from the concept of chemisorption bond formation. But Sample No. 2 shows an increase of magnetization and a shift of the resonance field to a higher value. This increase of magnetization can logically be explained as due to a decrease in anisotropy, as in the analogous case of the permeameter measurements (5, 6, 24). In the particles in Sample No. 2, which

exhibit a higher anisotropy, the decrease of anisotropy on adsorption of hydrogen permits more electrons to be in resonance, and this effect is greater, in its influence on the observed magnetization, than the simultaneous decrease of magnetic moment caused by formation of the chemisorption bond. At 250°C Sample No. 2 shows a decrease in magnetization after adsorption. This is due to the relatively smaller anisot-

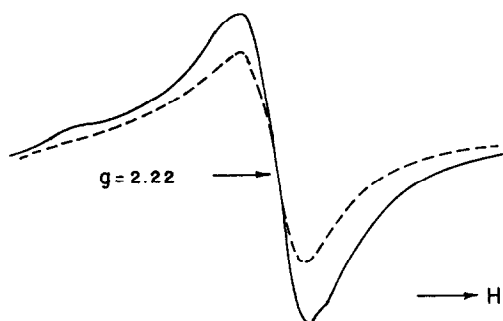


FIG. 5. FMR signal from Sample No. 1 at 25°C; —, evacuated, the linewidth is 550 gauss; - - -, treated with hydrogen,  $P(H_2) = 500$  mm Hg, the linewidth is 550 gauss.

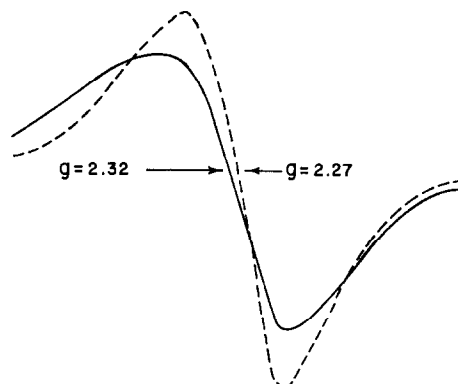


FIG. 6. FMR signal from Sample No. 2 at 25°C; —, evacuated, the linewidth is 1280 gauss; - - -, treated with hydrogen,  $P(H_2) = 500$  mm Hg, the linewidth is 1090 gauss.

ropy present at the more elevated temperature, so that a decrease of this anisotropy is then not sufficient to erase the decrease of magnetic moment. But in the smaller particles present in Sample No. 1 any anisotropy effect is too small to produce the anomaly of an increase of magnetization. Figure 7 shows the FMR spectra for Sam-

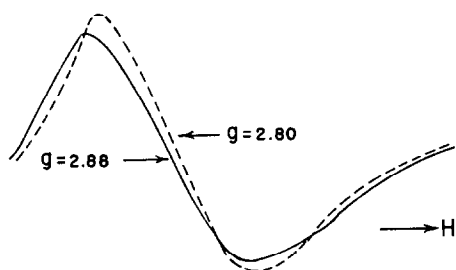


Fig. 7. FMR signal from Sample No. 2 sintered *in vacuo* 4 hr at 450°C; —, evacuated, the linewidth is 1420 gauss; - - - -, treated with hydrogen,  $P(\text{H}_2) = 500$  mm Hg, the linewidth is 1350 gauss.

ple No. 2 which had been sintered at 450°C and which, therefore, had still larger particles, greater anisotropy, and a further shift to higher  $g$  values both before and after adsorption of hydrogen.

**Adsorbed ethylene.** The influence of adsorbed ethylene at 25°C and 40 mm Hg is shown in Figs. 8 and 9 for Samples Nos. 1

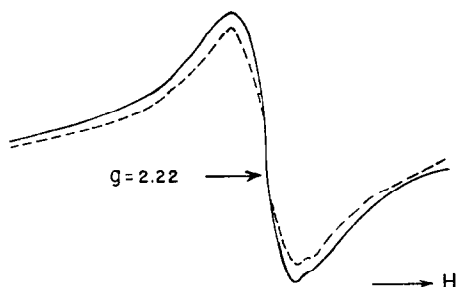


Fig. 8. FMR signal from Sample No. 1 at 25°C; —, evacuated, the linewidth is 550 gauss; - - - -, treated with ethylene,  $P(\text{C}_2\text{H}_4)$  40 mm Hg, the linewidth is 550 gauss.

and 2, respectively. The effect of the ethylene is sufficiently like that of hydrogen as to require no further explanation. It must, however, be pointed out that the mode of chemisorption of ethylene on nickel is

strongly dependent on experimental conditions (1).

**Adsorbed oxygen.** Figure 10 shows the influence of adsorbed molecular oxygen at 25°C and 50 mm Hg on Sample No. 1.

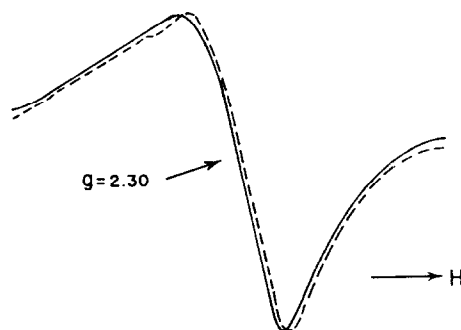


Fig. 9. FMR signal from Sample No. 2 at 25°C; —, evacuated, the linewidth is 1050 gauss; - - - -, treated with ethylene,  $P(\text{C}_2\text{H}_4)$  40 mm Hg, the linewidth is 1050 gauss.

There is, in this case, a decrease of magnetization caused by decoupling of the magnetic moments associated with those surface atoms engaged in forming the chemisorption bond from those atoms in the remainder of the metal particle (6). The

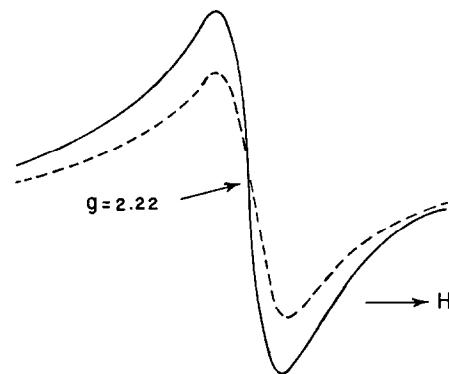


Fig. 10. FMR signal from Sample No. 1 at 25°C; —, evacuated, the linewidth is 500 gauss; - - - -, treated with oxygen,  $P(\text{O}_2)$  50 mm Hg, the linewidth is 500 gauss.

same effect is shown on Sample No. 2 in Fig. 11, but in addition there is a shift of the resonance position to a smaller value. On this sample the effect of oxygen is, therefore, different from that of hydrogen at the same temperature. This might be explained by a smaller influence of oxygen on the

magnetic anisotropy as compared with hydrogen. Another explanation is that resonance excitation may not be uniform with all spins parallel, but rather may exhibit a difference between surface spins and bulk spins, by the effect called "surface pinning." Theoretical treatment of line shape in the case of surface pinning (13) shows that it produces a shift in the resonance to lower

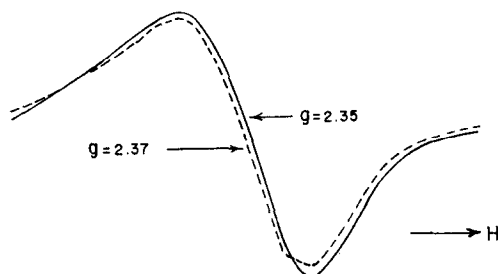


FIG. 11. FMR signal from Sample No. 2 at 25°C; —, evacuated, the linewidth is 1320 gauss; ----, treated with oxygen,  $P(O_2)$  50 mm Hg, the linewidth is 1320 gauss.

field values, a broadening of the line, and a lowering of the intensity, all of which were observed in the present case. The effect of surface pinning depends strongly on the value of the surface anisotropy constant,  $K_s$ . Of the various explanations for this found in the literature (26-28), two are possible in the present case.

First, surface pinning may be due to a difference in symmetry of nearest-neighbor surface atoms compared to similar atoms in the bulk (26). This explanation seems less probable in the present case because it should apply both to the hydrogen case and to the oxygen. Second, there may be formed an antiferromagnetic surface layer coupling the ferromagnetic surface spins under it (27). It is known that when molecular oxygen is adsorbed on nickel it penetrates under surface atoms (29), forming a thick layer of nickel oxide (30, 31) which causes surface pinning because of the anisotropy decrease. This effect need not, of course, occur if the oxygen is introduced to the metal surface in the form of nitrous oxide.

On nickel particles of small diameter the surface pinning and the effect of surface spin decoupling predominate. A decrease of

magnetization is thus observed, and a shift toward a smaller resonance field. But if the sample is sintered, the particle diameter increases and the decrease of magnetocrystalline anisotropy prevails over the surface pinning. In this case the magnetization increases after oxygen adsorption, as it does

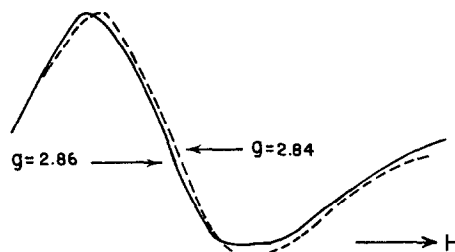


FIG. 12. FMR signal from Sample No. 2 sintered *in vacuo* 4 hr at 450°C; —, evacuated, the linewidth is 1400 gauss; ----, treated with oxygen,  $P(O_2)$  50 mm Hg, the linewidth is 1400 gauss.

for hydrogen on samples of similar particle size. This result, which is shown in Fig. 12, confirms the previously reported increase obtained by the constant-field method (1). It must be emphasized also that the admission of oxygen to a nickel surface generates sufficient heat to sinter small particles.

#### SUMMARY

It appears from this work that in spite of the complexities involved in ferromagnetic resonance, especially in the case of polycrystalline material (20), it is possible to gain a better understanding of surface and adsorption phenomena by this method. Although the precise nature of the nickel-hydrogen bond remains obscure, the effect of this bond on the magnetic properties of an assembly of nickel particles of various sizes and shapes is reasonably well accounted for. In the case of oxygen the more probable mechanism of adsorption involves the decoupling of surface atomic moments of nickel and the formation of an antiferromagnetic layer of nickel oxide as proposed by Geus and Nobel (6).

#### ACKNOWLEDGMENTS

This work was in part performed under grant from the Army Research Office (Durham). Grate-

ful acknowledgment is made to the Bulgarian Academy of Sciences for assistance given to A. A. Andreev. It is a pleasure also to acknowledge the aid received from Dr. Douglas C. McCain in connection with the EPR work.

## REFERENCES

1. SELWOOD, P. W., "Adsorption and Collective Paramagnetism." Academic Press, New York and London, 1962.
2. BROEDER, J. J., VAN REIJEN, L. L., AND KORSWAGEN, A. R., *J. Chim. Phys.* **54**, 37 (1957).
3. HOLLIS, D. P., AND SELWOOD, P. W., *J. Chem. Phys.* **35**, 378 (1961).
4. LOY, B. R., AND NODDINGS, C. R., *J. Catalysis* **3**, 1 (1964).
5. LEAK, R. J., AND SELWOOD, P. W., *J. Phys. Chem.* **64**, 1114 (1960).
6. GEUS, J. W., AND NOBEL, A. P. P., *J. Catalysis* **6**, 108 (1966).
7. VAN EIJK VAN VOORTHUIJSEN, J. J. B., AND FRANZEN, P., *Rec. Trav. Chim.* **70**, 793 (1951).
8. GRIFFITHS, J. H. E., *Nature* **158**, 670 (1946).
9. SELWOOD, P. W., ADLER, S., AND PHILLIPS, T. R., *J. Am. Chem. Soc.* **77**, 1462 (1955).
10. RUBINSHTEIN, A. M., YOST, F., AND SLINKIN, A. A., *Izv. Akad. Nauk SSSR, Ser. Khim.* (No. 2), p. 2481 (1964).
11. BLOEMBERGEN, N., *Phys. Rev.* **78**, 572 (1950).
12. REICH, K. H., *Phys. Rev.* **101**, 1647 (1956).
13. ROBBELL, D. S., *Physics* **1**, 279 (1965).
14. YASUMURA, J., *Nature* **207**, 5002 (1965).
15. SLINKIN, A. A., AND PAPER, E., *Dokl. Akad. Nauk SSSR* **158**, 1405 (1964).
16. TUROV, E. A., in "Ferromagnetic Resonance" (S. V. Vonsovskii, ed.). Pergamon Press, New York, 1966.
17. SCHLOMANN, E., *Phys. Chem. Solids* **6**, 242 (1958).
18. SCHLOMANN, E., *Phys. Chem. Solids* **6**, 257 (1958).
19. SKROTSKII, G. V., AND KURBATOV, L. V., in "Ferromagnetic Resonance," p. 30. Pergamon Press, New York, 1966.
20. VONSOVSKII, S. V., in "Ferromagnetic Resonance," p. 1. Pergamon Press, New York, 1966.
21. JANKO, A., *Naturwissenschaften* **47**, 225 (1960).
22. BONISZEWSKI, T., AND SMITH, G. C., *Phys. Chem. Solids* **21**, 115 (1960).
23. WOLLAN, E. O., CABLE, J. W., AND KOEHLER, W. C., *Phys. Chem. Solids* **24**, 1141 (1963).
24. DIETZ, R. E., AND SELWOOD, P. W., *J. Chem. Phys.* **35**, 270 (1961).
25. GEUS, J. W., NOBEL, A. P. P., AND ZWIETERING, P., *J. Catalysis* **1**, 8 (1962).
26. NÉEL, L., *J. Phys. Radium* **15**, 225 (1954).
27. MEIKELJOHN, W. H., AND BEAN, C. P., *Phys. Rev.* **102**, 1413 (1965); MEIKELJOHN, W. H., AND BEAN, C. P., *Phys. Rev.* **105**, 904 (1957); MEIKELJOHN, W. H., *J. Appl. Phys.* **29**, 454 (1958).
28. WIGEN, P. E., KOOL, C. F., SHANNABARGER, M. R., AND ROSSING, T. D., *Phys. Rev. Letters* **9**, 206 (1962).
29. KIPERMAN, S. L., AND DAVJDOVA, J. R., *Kinetika i Kataliz* **2**, 762 (1961).
30. DELL, R. M., KLEMPERER, D. F., AND STONE, F. S., *J. Phys. Chem.* **60**, 1586 (1956).
31. KLEMPERER, D. F., AND STONE, F. S., *Proc. Roy. Soc. (London)* **A243**, 375 (1957).